Sensors and Actuators A 212 (2014) 25–33

Contents lists available at ScienceDirect

Sensors and Actuators A: Physical

journal homepage: www.elsevier.com/locate/sna

Localization and velocity tracking of human via 3 IMU sensors

Qilong Yuan*, I-Ming Chen[1]

School of Mechanical and Aerospace Engineering, Nanyang Technological University, Nanyang 50, RRC, Singapore 597627, Singapore

ARTICLE INFO

Article history:
Received 23 October 2013
Received in revised form 3 March 2014
Accepted 4 March 2014
Available online 21 March 2014

Keywords:
Human velocity tracking
IMUs
Inertial sensors

ABSTRACT

In sports training and exercises like walking and jogging, the velocity and position of the exercise people is very crucial for motion evaluation. A simple wearable system and corresponding method for velocity monitoring using minimal sensors can be very useful for daily use. In this work, a velocity tracking and localization method using only three IMU sensors is introduced. The three sensors are located at the right shank, right thigh and the pelvis to measure the kinematics of the lower limbs. In the method, a reference root point on the pelvis is chosen to represent the velocity and location of the person. Through acceleration fine tuning algorithm, the acceleration data is refined and combined with the velocity calculated from body kinematics to get a drift-free and accurate 3D velocity result. The location of the person is tracked based on this velocity estimation and the limb kinematic subsequently. The benchmark study with the commercial optical reference shows that the error in velocity tracking is within 0.1 m/s and localization accuracy is within 2% in both normal walking, jogging and jumping. Due to the conveniences of the small-size wearable IMU sensors, this proposed velocity tracking and localization method is very useful in everyday exercises both indoor and outdoor.

1. Introduction

Tracking the human motion and the physical human–environment interaction via wearable sensors closely relies on the human body kinematics, kinetics, and the contact interactions with the environment. Among the large amount of parameters of human motion, the awareness of velocity and location of human is very important for applications like sports training, exercises and entertainment etc. In daily applications, the human subject usually acts in house or an open environment. Although additional infra-structure localization devices such as ultrasonic, radio frequency identification (RFID) and ultra-wideband (UWB) etc. can be installed in the surroundings for localization, in these sports and exercises related applications which take place in large areas, they are not economically viable. The GPS system is not precise enough for positioning accuracy below one meter and it is normally only available in open outdoor environments. In these daily applications, it is expected to use simple wearable sensors to track the location and velocity of the person without depending on external infra-structures. The wireless IMUs (inertial measurement units) wearable sensors are small and do not have the capture volume limitations. Therefore, they now show a great advantage to be widely applied in many daily motion tracking applications [1–4]. Existing IMU based motion captures systems use many sensors (usually more than 10) to track the human motion data. In many applications where the full body motions are not concerned, methods and system with minimal sensors to track the key kinematic information of interests are necessary.

In sports training such as walking, heel-to-toe walking and jogging, monitoring the velocity is quite crucial to study the efficiency of the exerciser. The speed of a subject describes how fast and in which direction the person moves in space. Also, its integration provides an update of the location data. Therefore, tracking the human moving velocity using wearable sensor is very helpful for such applications.

Theoretically, root point velocity can be estimated by integrating the acceleration of the root point over a period of time. However, the slight acceleration errors [5] measured by the IMUS will lead to unbounded drifting errors in just a few seconds [6]. Thus, direct integration of the acceleration is not suitable for velocity tracking of daily applications. Simple model based methods [7] only provide an average velocity estimation and is not generally accurate for different walking speeds. In gait study and personal navigation, researchers use the foot-mounted IMU sensors to track the foot location and velocity [8–11]. Among these methods, the ZUPTs algorithm is efficient for regular walking localization, where the foot velocity is also tracked while walking. Since the foot velocity is zero when it stance on the floor, it cannot provide

* Corresponding author. Tel.: +65 98965107.
E-mail addresses: yu0017ng@e.ntu.edu.sg (Q. Yuan), michen@ntu.edu.sg (I.-M. Chen).
[1] Tel.: +67906203.

http://dx.doi.org/10.1016/j.sna.2014.03.004
0924-4247/

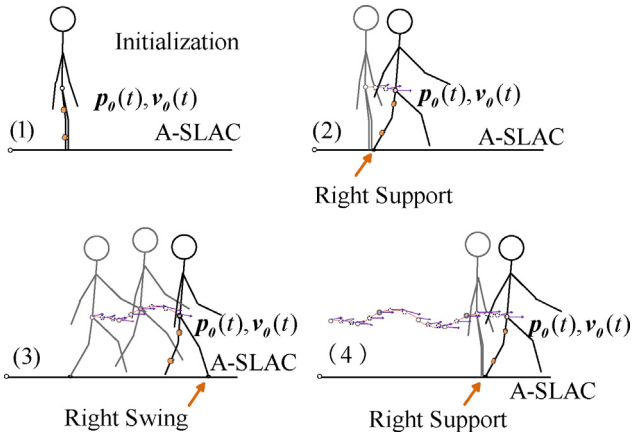

Fig. 1. Working principle of A-SLAC.

the continuous body velocity during motion. Also, during dynamic behaviors with obvious contacts, the large acceleration error will increase the velocity tracking and localization error in this method.

Therefore, to better resolve this velocity tracking issue, new methods for the inertial sensor to track the general practical moving velocity and location is expected.

In the previous work, we developed an IMU sensors based motion capture system with velocity and location tracking capability [3,4,12,13]. With calibrated skeleton model [14], contact phase detection, the 3D velocity, location and motions of the subject when the person walks, climbs up/down stairs etc. are tracked. The previous method is name as velocity based simultaneous localization and capture, V-SLAC. Eight IMUs were used in the early method.

In many application scenarios, people only concern about the trajectory and the moving speed of the subject. For example, in personal localization and jogging, the location and the velocity are the key parameters. In this case, it would be good if the system can have as few sensors as possible. Therefore, we started the work in this paper to improve the method through using only three IMUs for tracking.

In [3], the velocity of the root point is calculated based on the leg kinematics every time the right or the left foot contacts the ground. Therefore, wearable sensors on both legs are needed to track the kinematic parameters for the root velocity calculation. The velocity tracking during the non-contact phase comes from the integration of the root acceleration over time. Because of the root acceleration errors in the sensor measurement, the integration update on the velocity drifts gradually over time. Therefore, the reference velocity from the lower limb kinematics should show up frequently for every step in order to prevent large drifting errors in the velocity.

In this paper, the idea is that if the error of the root acceleration can be estimated and eliminated, the integrated root velocity result can be more reliable so that we can track only one leg's kinematics for the velocity update. In this case, the number of sensors for the tracking system will reduce. Thus, in this proposed method, the acceleration error is estimated based on calculating the drifting rate of the velocity. Subsequently, the acceleration error is fine tuned to eliminate the drifting effect.

The method is illustrated in Fig. 1. (1) Initially, the sensors and the limb lengths are calibrated. The initial position and velocity of the person is registered. (2) As the subject start to move, the shoe pad detect the right contact phase (sensors are mounted on right legs). The location and the velocity of the person are updated, and the acceleration of the subject is also updated as well. (3) When the right contact is not available, the velocity and location of the person are updated based on the integrations of the refined acceleration.

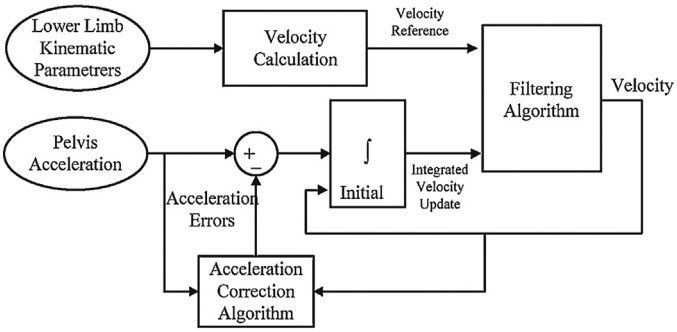

Fig. 2. Velocity tracking algorithm.

(4) The whole capture cycle repeats. This method is name as acceleration based simultaneous localization and capture, A-SLAC.

The remaining parts of the paper are organized as follow: Section 2 introduces the velocity tracking and localization algorithm. Section 3 introduces the system devices. Section 4 shows the experimental results. Finally, Section 5 concludes this paper.

2. Velocity tracking

In this system, the root point is located around the center of the pelvis [6,13] and an IMU is placed there to measure the root acceleration. The velocity of the body can be estimated based on the limb kinematics and the contacting foot. As shown in Fig. 2. This velocity solves as a reference to (1) correct the acceleration errors and (2) fuse with the integration update through a Kalman filter to achieve reliable velocity results.

2.1. Calibration

Prior to the experiments, this system undergoes the calibration processes to identify several important kinematic parameters of the limbs. First, the coordinate mappings between the local frames and the limb body frames is calibrated so that sensor data collected in the local frames can be transformed into the limb body frames accurately [12].

Second, the limb dimensions of the person need to be calibrated to define the kinematics of the lower limbs. In case of 3 IMU sensors, the dimensions of limbs are estimated using direct measurement on the limb lengths, the accuracy of this estimation in limb lengths is within 2 cm.

2.2. Contact phase detection

The purpose of contact phase detection is to detect the foot contact event so that the root velocity can then be estimated from the supporting foot. Four FSR force sensors are arranged in the shoe pad and serve as a contact switch to indicate the impact and stationary phase of the (right) foot. In case of contact, the reference velocity will be introduced to correct the velocity when the right foot contacts the floor.

For exercises like walking, jogging, heel-to-toe walking and jumping etc., the right foot contact will regularly appear within every second. Therefore, the reference velocity will regularly contribute to correct the velocity updates.

2.3. Velocity tracking

In this method, an IMU sensor is attached to the root point to measure the root acceleration [15]. Inertial sensors can measure the angular velocity of the body limbs. Therefore, based on the velocity kinematic model of human body, the velocity of the root point can

be estimated. This reference velocity can be combined with the integration of the root acceleration through a Kalman filter to obtain accurate and drift-free velocity value. Subsequently, the location of the person can be tracked based on the time integration of this velocity update and kinematic calculations as discussed in V-SLAC. In this manner, the localization of the dynamic motions with non-contact phases such as jumping and jogging can also be realized [3,4].

The pelvis IMU, which is attached to the root point, measures the root acceleration a_f (with gravity included) in the sensor frame. Thus, the root acceleration a_r with respect to the global reference can be obtained by transforming the accelerometer measurement from the body frame to the global frame, and eliminate the gravitational acceleration

$$a_r = R_{0S} a_f - g, \tag{1}$$

where R_{0S} denotes the measured orientation of the pelvis IMU.

Then, the root velocity v_k can be updated based on integration over time, with dt being the time interval:

$$v_k = v_{k-1} + \mathrm{d}t \cdot a_r. \tag{2}$$

Let δR_{0S} denotes the orientation error in the measurement and let δa_f denotes the white noise of the accelerometer measurement. Then, the error of the accelerations can be calculated by

$$\begin{aligned} \delta a_r &= \delta R_{0S} R_{0S} \left(a_f + \delta a_f\right) - R_{0S} a_f \\ &\approx \left(\delta R_{0S} - I\right) R_{0S} a_f + R_{0S} \delta a_f \\ &= \delta a + R_{0S} \delta a_f, \end{aligned} \tag{3}$$

where $\delta a = \delta\hat{\omega}_0 R_{0S} a_f = -(R_{0S} a_f\hat{)}\delta\omega_0$, where $\delta\omega_0$ (3×1) denotes the corresponding angular vector of δR_{0S}, $\delta R_{0S} = e^{\delta\hat{\omega}_0} \approx I + \delta\hat{\omega}_0$. Then, we know the property of the acceleration noise which will be useful while combining the acceleration update with the velocity estimated from the velocity kinematics using a Kalman filter.

2.3.1. The Kalman filter for velocity tracking

In the velocity update based on the integration of acceleration with time as shown in Eq. (2), the discrete-time controlled process to estimate the state is governed by the following difference equation,

$$v_k = A_v v_{k-1} + B_v a_{r,k-1} + W_k w_{k-1}, \tag{4}$$

where v_k denotes the velocity, $a_{r,k-1}$ denotes the root acceleration and w_k denotes the white noise. Thus, according to Eqs. (2) and (3), we have:

$$A_v = I_{3\times 3}, \quad B_v = \delta t \cdot I_{3\times 3}, \quad W_k = \left[-(R_{0S} f\hat{)}, R_{0S}\right].$$

$$w = \left[\delta\xi_0{}^T, \delta a_f{}^T\right]^T$$

On the other hand, when a foot stationary phase is detected, the velocity of the root can be estimated from the kinematic chain of the supporting leg based on the velocity kinematics.

As shown in Fig. 3, when the foot is stationary, the ankle velocity becomes zero. The root velocity can be calculated based on the motion of the shank, the thigh and the pelvis. Thus the measured velocity v_m based on velocity kinematics of the root is

$$v_m = -\sum_{i=0}^{2} R_i \left(\omega_{i,b} \times l_{i,i+1}\right). \tag{5}$$

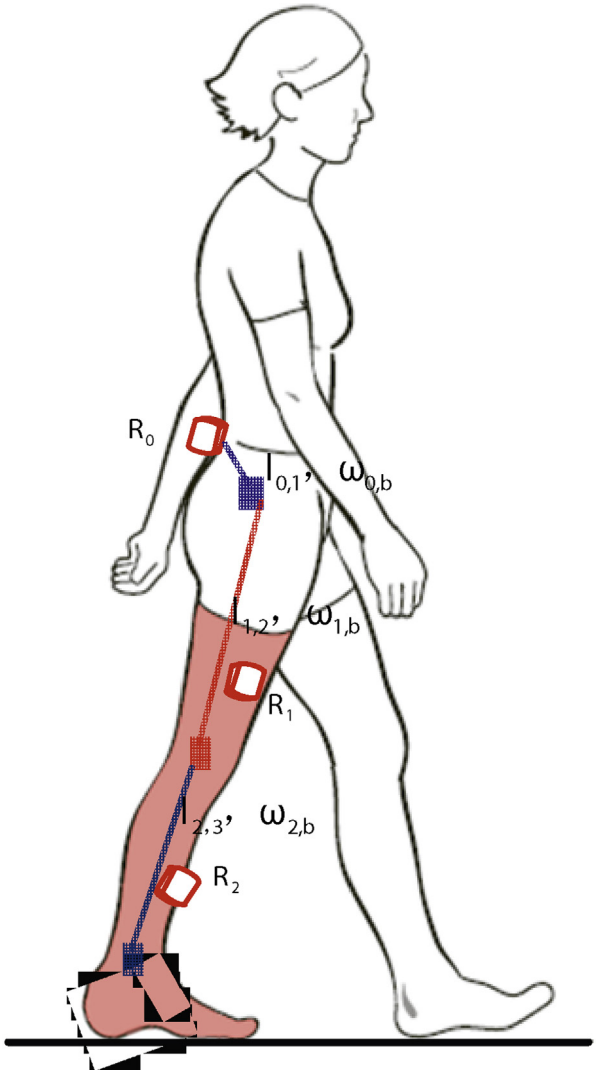

Fig. 3. Postures before and after refinement.

For the existence of uncertainties in limb length and sensor measurements, the reference velocity from this kinematic calculation is represented as follows

$$v'_m = -\sum_{i=0}^{2} \left[\delta R_i \times R_i \left(\omega_{i,b} + \delta\omega_{i,b}\right) \times \left(l_{i,i+1} + \delta l_{i,i+1}\right)\right], \tag{6}$$

where δR_i denotes the orientation errors which corresponds to an angular error $\delta\theta_i$ and $\delta R_i = e^{\delta\hat{\theta}_i} \approx I + \delta\hat{\theta}_i$. The angular rate white noise is denoted by $\delta\omega_{i,b}$, and $\delta l_{i,i+1}$ denotes the uncertainty of the limb dimensions.

Referring to Eqs. (5) and (6), we have

$$\delta v_m = v'_m - v_m = V \upsilon_k. \tag{7}$$

where $V = [V_1, V_2, V_3]$,

$$\upsilon_k = \left[\delta\theta_1^T, \delta\omega_1^T, \delta l_{0,1}^T, \delta\theta_2^T, \delta\omega_2^T, \delta l_{1,2}^T, \delta\theta_3^T, \delta\omega_3^T, \delta l_{2,3}^T\right]^T,$$

and

$$V_i = -\left[(-R_i(\omega_{i,b} \times l_{i,i+1})\hat{)}, (-R_i l_{i,i+1}\hat{)} \times R_i, (R_i\omega_{i,b}\hat{)} \times R_i\right]$$

2.3.2. SLAC with acceleration fine tuning (A-SLAC)

The working principle of the acceleration fine tuning is illustrated in Fig. 2. The pelvis IMU is mounted at the root point to measure the root point acceleration and the pelvis motion. When

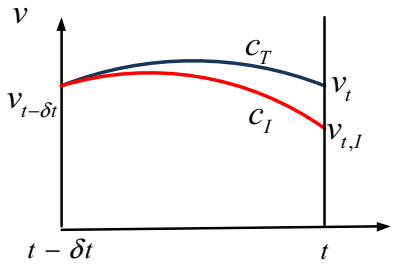

Fig. 4. Velocity drifting illustration.

the foot (of the leg with sensors) stands on the ground, the velocity of the root point can be accurately tracked based on V-SLAC as discussed in Section 2.3. On the other hand, integration of the root point acceleration provides another velocity value that has the drifting errors. Comparing these two velocities can provide the drifting rate of the integrated velocity, which is the acceleration error.

As illustrated in Fig. 4, the true velocity of the root point is represented as a blue curve c_T. The velocity obtained from integrating the measured acceleration is plotted as a red curve c_I. The acceleration error is the drifting rate of the integrated velocity during this short period δt.

$$\delta a = \frac{v_t - v_{t,I}}{\delta t} \tag{8}$$

It is reasonable to assume that during a very short period of time δt, (for example with the sampling rate of 50 Hz, within 25 samples 0.5 s), the acceleration error does not change much. Thus, the acceleration error can be estimated by determining the drifting rate of the velocity in this period of time.

Referring to Eq. (4), after fine tuning the root point acceleration, the discrete-time controlled process to estimate the velocity is governed by the following difference equation:

$$\begin{aligned} v_k &= v_{k-1} + \left(a_{rm} - \delta a\right) \cdot \delta t + \left(\delta t \cdot R_r\right) \delta a_f \\ &= A_A v_{k-1} + B_A u_{k-1} + W_A w_{k-1} \end{aligned} \tag{9}$$

where $A_A = I_{3\times3}$, $B_A = \delta t \cdot [I_{3\times3},\ I_{3\times3}]$, $W_A = \delta t \times R_r$, and $u_k = [a_{rm,k}^T, -\delta a_{r,k}^T]^T$.

Q_w represents the covariance of the white noise of the accelerometer measurement δa_f.

Let the estimated root acceleration be $a_{r,m} = \delta a_r + a_r$. The true acceleration is denoted by a_r and the acceleration error is δa_r.

Then according to Fig. 4, we have:

$$\int_{t-\delta t}^{t} a_{r,m} dt = \int_{t-\tau}^{t} \left(\delta a_r + a_r\right) dt = \delta a_r \delta t + (v_t - v_{t-\tau}) \tag{10}$$

Thus

$$\delta a_r = \frac{\int_{t-\tau}^{t} a_{r,m} \mathrm{d}t - (v_t - v_{t-\tau})}{\delta t}. \tag{11}$$

In the discrete-time process, the acceleration error can be estimated in every n samples by

$$\delta a_{r,k} = \frac{\sum_{i=k+1-n}^{k} a_{r,m,i} \mathrm{d}t - (v_k - v_{k+1-n})}{n \mathrm{d}t}. \tag{12}$$

2.3.3. Velocity fusion

According to Eq. (7), we have the velocity measurement z_{vk} estimated from the limb kinematics as below:

$$z_{vk} = v_m = v'_m - V\upsilon_k = H_v v_k + V_v \upsilon_k, \tag{13}$$

where $H_v = I_{3\times3}$, and $V_v = -V$.

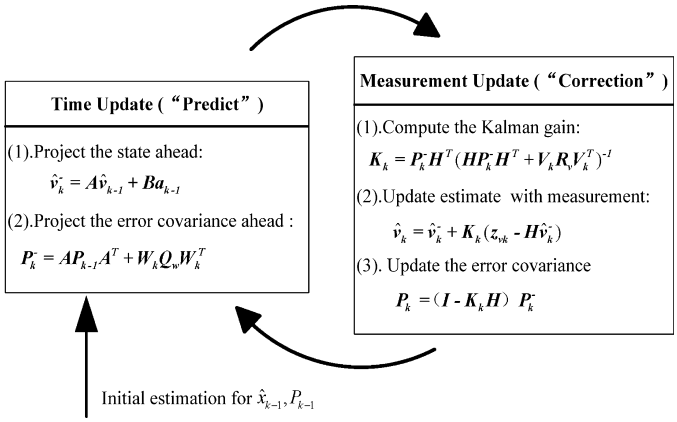

Fig. 5. Velocity tracking Kalman filter.

In this model, the accelerometer and gyroscope measurement errors are white noises. The angular error and the skeleton dimension errors are approximated to be normally distributed with certain uncertainties in the skeleton dimension model. In this way, $p(w) = N(0, Q_w)$; $p(\upsilon) = N(0, R_v)$. Referring to the specification of the sensors [16,17] and the kinematic uncertainty, the process noise covariance matrix of Q_w and R_v are determined.

Based on Eqs. (4) and (13), the velocity can be updated using the introduced Kalman filter algorithm as shown in Fig. 5 [18,19].

2.4. Velocity based localization (V-SLAC)

In A-SLAC, during the contact phases, the location updated based on SLAC can be combined with the root velocity integration to update the subject's spatial location. Thus, a Kalman filter can combine these two location estimations together to provide localization update. In the non-contact phases, the location is estimated by the integration of the velocity estimation over time. Fig. 6 shows the working flow of the localization. The dashed-line in Fig. 6 means that these references are only available during the contact phases.

In A-SALC, the stride vector is used as the state variables. The final location is calculated based on summing up all the stride vectors from the beginning to the end. Unlike walking where the steps

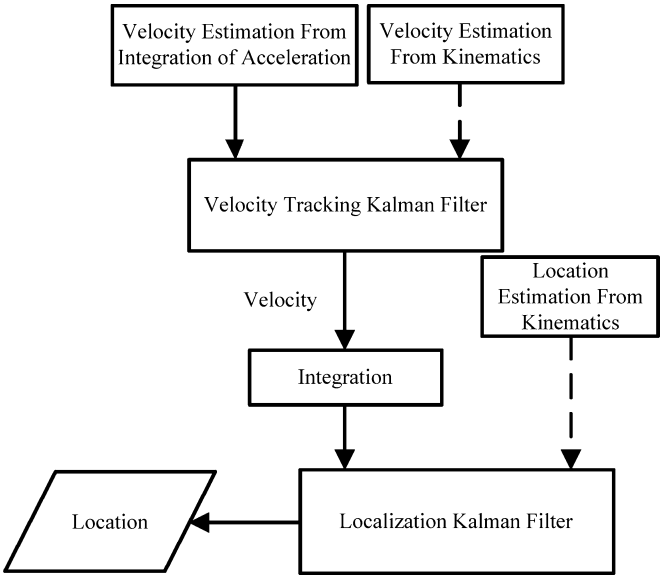

Fig. 6. Fusion algorithm for localization.

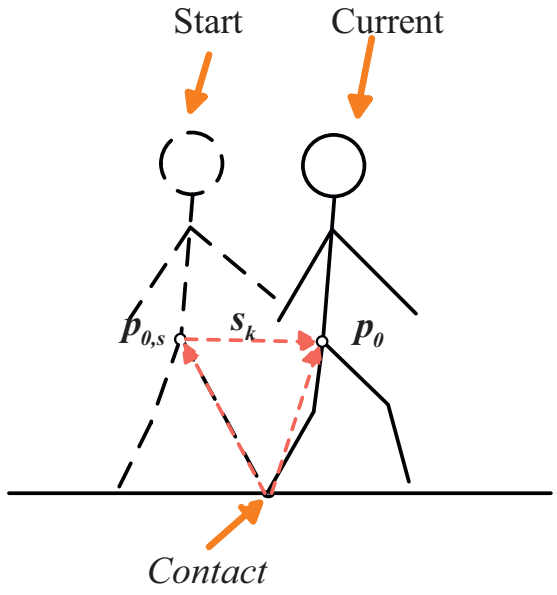

Fig. 7. Stride vector estimated from kinematics.

are clearly defined based on the gait phases, the stride vector s_k in A-SLAC is defined in such a way that it starts from the beginning of a foot support phase, and ends at the beginning of a new foot support phase as illustrated in Fig. 7.

In the root location update based on the integration of the root velocity over time, the discrete-time controlled process to estimate the state variable (s_k) is governed by the following difference equation

$$s_k = A_s s_{k-1} + \mathrm{d}t \cdot v_{0,k-1} + w_{s,k-1}, \tag{14}$$

or

$$s_k = A_s s_{k-1} + B_s v_{0,k-1} + w_{s,k-1}, \tag{15}$$

where $A_s = I_{3\times3}$, $B_s = \mathrm{d}t \cdot I_{3\times3}$, and $w_{s,k}$ denotes the white process noise caused by the noise of the input velocity: $p(w_s) = N(0, Q_s)$. With the known error covariance matrix P_k of velocity input as shown in Section 2.3, the process noise covariance in Eq. (14) is $Q_{s,k} = \tau^2 P_k$.

On the other hand, the stride vector measurement is available based on the lower limb kinematics during the foot support phases (see Fig. 7):

$$z_{s,k} = s_{m,k} + \vartheta_k, \quad P(\vartheta_k) \sim N(0, R_{s,k}). \tag{16}$$

where ϑ_k denotes the measurement noise and the noise covariance is $R_{s,k}$ which can be calculated based on the kinematic uncertainty. Then the stride vector can be combined based on Eqs. (15) and (16) using Kalman filter in Fig. 8.

After updating the step vector s_k, the root location can be calculated as follows.

$$p_0 = p_{0,s} + s_k, \tag{17}$$

where $p_{0,s}$ denotes the location of the root point at the starting moment of current step.

During the non-contact phase, only the left half of the Kalman filter is applied to update the stride vector value and also the covariance matrix $P_{s,k}$. In this manner, the spatial location of the human during both contact phases and non-contact phases can be captured continuously based on this method.

Note that the velocity reference is only available for the leg with sensors during the foot contact. If the subject exercises the leg without sensors for a long time without letting the leg with sensors

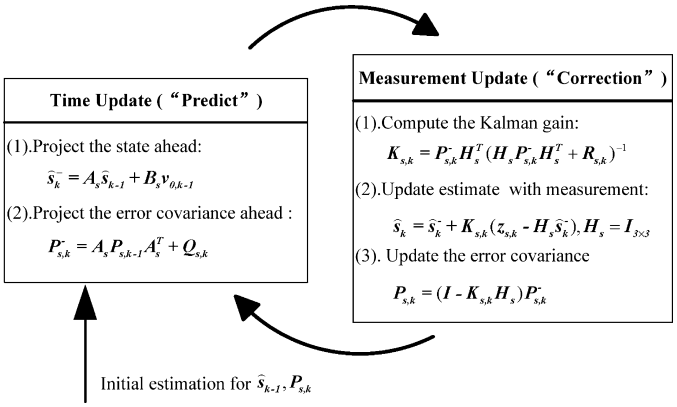

Fig. 8. Localization Kalman filter in V-SLAC.

touching the ground, A-SLAC cannot work. This is one limitation of this method as compared with the SLAC and V-SLAC method.

3. System devices

As shown in Fig. 9, the velocity and position tracking system consists of three inertia measurement units (IMU) sensors and a sensitive shoe pad. The commercial IMUs (APDM®, US) are used to measure the spatial orientation of the object and other kinematic quantities including angular velocity and accelerations. The insoles of the shoes are used to identify the foot contacts. Four force sensing resistors (FSR) with the controllers are fabricated in the insole shoe pad to detect the contact phases. Details can be found in [3]. All the sensors data are wirelessly sent to a mobile device. The transmission range of the sensors is 10 m line of sight. Currently, we use a laptop to collect the data. It could be implemented with a smart phone in the future such that the users can directly view their real time speed and other kinematic parameters like distance of travel, average velocity etc.

The system can be easily worn one the body with little constraint of the human body movements. The IMUs are tightly attached on the limbs to minimize the effect of the skin and muscle effects. For these advantages with these small-size potable IMUs, the applications like walking, jogging, heel-to-toe walking, and jumping etc. can be tracked easily within various applications.

The specifications of the IMU sensors are listed in Table 1. To get drift-free orientation estimation, instead of collecting orientation result from the sensor, we used the raw data from the

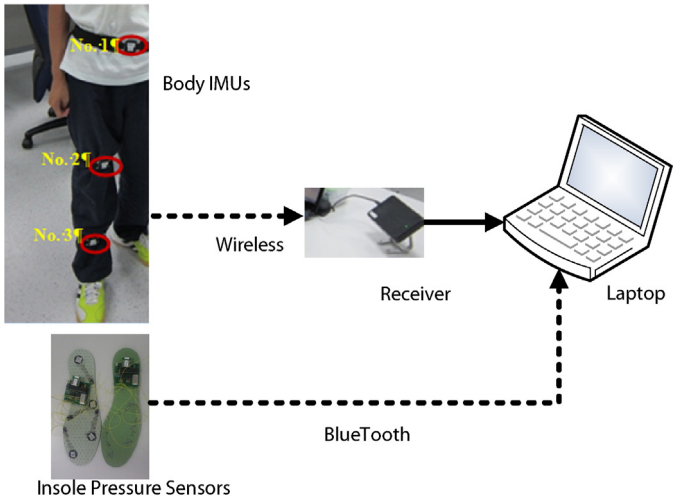

Fig. 9. System setup.

Table 1
Sensor characteristics.

Item	Accelerometer	Gyroscope	Magnetometer
Axes	3 axes	3 axes	3 axes
Range	±6 g	±2000 deg/s	±6 Gauss
Noise	0.0012 m/s^2/$\sqrt{}$Hz	0.05 deg/s/$\sqrt{}$Hz	0.5 mGauss/$\sqrt{}$Hz

3 axes accelerometer, gyroscope and the magnetometers to update the orientation. The details of the tracking algorithm are not discussed here in this paper. For details, we can refer to [20,21]. The orientation error (along all directions) can be maintained at about 1 deg for slow motions, and 3 deg for motions like jumping and jogging.

4. Experimental results

To validate the A-SLAC method in velocity tracking and localization, a benchmark study with the *Opti-Track Motion Capture System* is conducted for jumping and jogging motions. To test the A-SLAC accuracy in outdoor, an A-SLAC experiment is conducted around the outside of the laboratory (53.6m × 16 m). It is understandable that this method is not affected by the moving pattern of different subjects, and the body sizes of subjects are considered in the model. Therefore, we only tested on one subject in this paper (Fig. 10).

4.1. Benchmark study of A-SLAC

In benchmark study of A-SLAC, the devices are:

(1) The Optical Motion Capture system has eight cameras. After the system calibration the marker position accuracy is about 0.3 mm.
(2) Three IMU sensors and one pair of insole shoe pad. The experiment procedures are as follows.

Fig. 10. System setup for benchmark study.

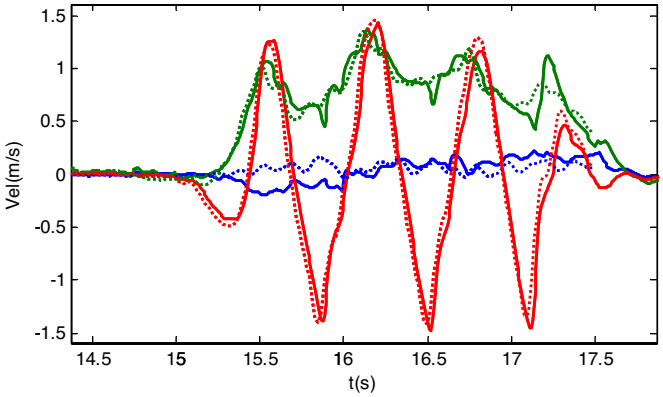

Fig. 11. Benchmark study of A-SLAC: root velocity. (For interpretation of the references to color in this figure legend, the reader is referred to the web version of this article.)

Step 1: The subject wears the three IMUs and attaches the reflective marker as reference.
Step 2: The optical system is calibrated.
Step 3: The wearable IMU sensors is calibrated.
Step 4: The subject jumps forward for three steps and walks back to the initial location.
Step 5: The subject repeats step 4 for five more times.
For the limitation of space in the lab, the benchmark area is relatively small.

4.1.1. Velocity result in A-SLAC

The motions are captured by the wearable tracking system and the optical capture system simultaneously. The position of the marker attached at the root point serves as a reference of the human subject. The derivative of the position value with respect to time serves as a velocity reference to evaluate the velocity accuracy of A-SLAC. As the reference coordinates used by the two capture systems are different, a coordinate transformation between the two is needed to unify the data in order to compare in the same global frame [3]. In this benchmark study, the reference frame is chosen to be the reference frame of the optical system.

Fig. 11 shows part of the result of the velocity from A-SLAC and the reference velocity in all directions. The reference velocity is represented as a dashed-line whereas the velocity from A-SLAC method is represented as a solid line (*X*-axis is in blue color, *Y*-axis is in green color, *Z*-axis is in red color).

The RMS errors of the velocity along all directions are calculated from the RMS of the difference between the results from the two systems along all the time samplings. The RMS error in the main walking direction (*Y*-axis direction) is 0.051 m/s, which is within 3% of the maximum velocity (1.5 m/s). The RMS error for the vertical direction is 0.029 m/s. In the lateral direction (blue), the result is less accurate (0.13 m/s).

4.1.2. Localization result using A-SLAC

Fig. 12 shows the corresponding localization results in all *X*-, *Y*-, *Z*-directions (the unit is meter). The reference root position is represented as the dashed-line whereas the velocity from A-SLAC is represented as a solid line (*X*-axis is in blue, *Y*-axis is in green, *Z*-axis is in red). In this experiment, the terrain is even ground. Therefore, the Z-coordinate of the supporting foot is set to be the same as the ground during the localization. In this manner, the drifting error in the vertical direction is prevented.

The RMS error shows the difference between the captured location trajectory and the reference trajectory for all the sample time. The RMS error in the main walking direction *Y*-axis is 3.8 cm (each trial is 3.6 m in length). The RMS error for the vertical direction is

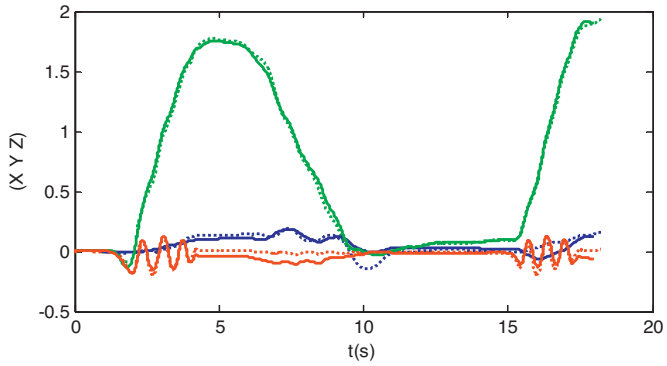

Fig. 12. Benchmark study of A-SLAC: root position. (For interpretation of the references to color in this figure legend, the reader is referred to the web version of this article.)

3.2 cm. In the sideway (Y) direction, the error is 5.7 cm, about 2% of the trial length.

4.2. Outdoor experiment of A-SLAC

In order to test the method and system for outdoor localization, the subject conducted an outdoor experiment around the room as shown in Fig. 13. The experiment procedures are as follows.

Step 1: The subject wears the 3 IMUs + the Shoe Pad, and calibrates the system at the starting location as shown in Fig. 13.

Step 2: The subject walks around the outside of a room (16 m × 53.6 m) and goes back to the starting point.

Step 3: The subject repeats Step 2 for three more times.

The map of the room shown in Fig. 13 provides a reference to evaluate the localization accuracy. The estimated travelled distance for one loop is about 170 m. Fig. 14 illustrates the root point 3D velocity and the trajectory of a sample path in the experiment while walking around the room. In the velocity plot on the top, the blue line represents the velocity in X-axis direction. The green line represents the velocity in Y-axis direction. The red line represents the velocity in Z-axis direction.

For the four trials conducted, the position error after returning to the starting point are $(x, y) = (1.59, 0.91)$ m, $(1.08, 0.77)$ m, $(1.18, 1.09)$ m, $(0.95, 0.83)$ m. This is within 2% of the total travelled distance. The absolute velocity error in this experiment is not available because there is no velocity reference in this experiment.

4.3. Jogging

In the jogging exercise, the velocity and the jogging distance are very important parameters to quantify the amount of exercise. A jogging experiment is conducted using this system. First we measure a distance of 7.5 m and mark the starting and ending position (this distance is short because the experiment is indoor since the power source is needed for the APDM sensor and receiver setup). The jogging tracking experiment procedures are as follows.

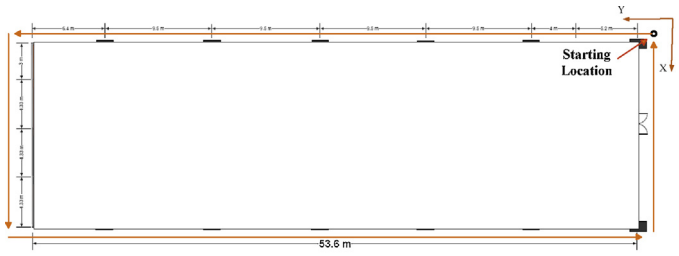

Fig. 13. Floor map for A-SLAC localization experiment.

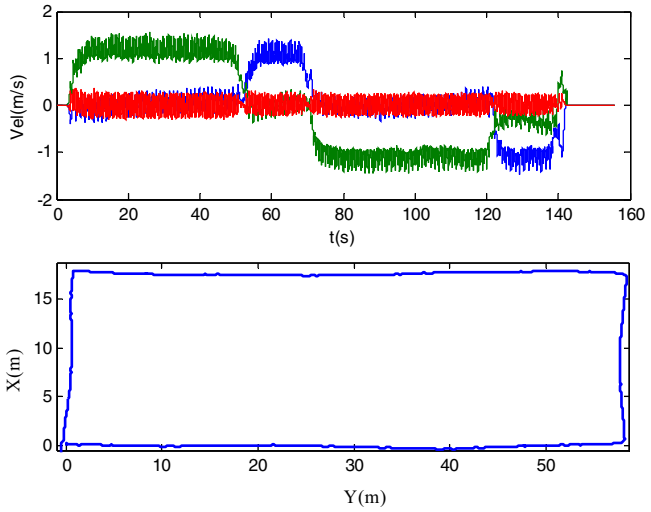

Fig. 14. Outdoor localization. (For interpretation of the references to color in this figure legend, the reader is referred to the web version of this article.)

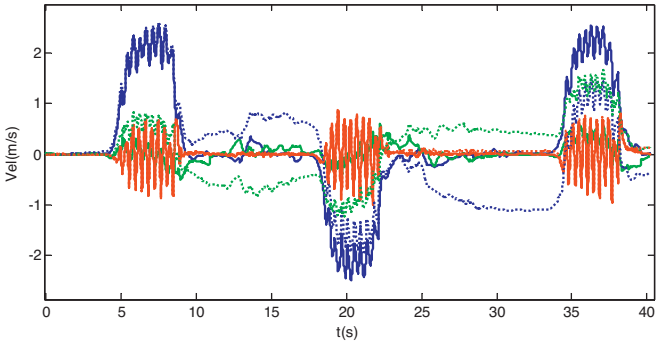

Fig. 15. Jogging velocity. (For interpretation of the references to color in this figure legend, the reader is referred to the web version of this article.)

Step 1: The subject calibrates the system in an initial starting position.

Step 2: The subject jogs for 7.5 m at the speed of 2 to 3 m/s to the ending position and then jog back to the starting location.

Step 3: The subject repeat Step 2 for three more times in the experiment.

The reference frame is defined as follows. The X-axis is in the north direction, the Z-axis is in the upward direction. The Y-axis is defined according to the right-hand rule. Figs. 15 and 16 show the tracked velocity and location results (X-axis is in blue, Y-axis is in green, Z-axis is in red). The dashed-line denotes the results from integration of the root acceleration. The solid line denotes the results from A-SLAC method.

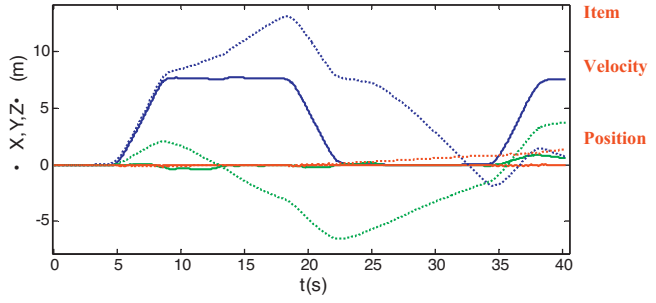

Fig. 16. Jogging localization. (For interpretation of the references to color in this figure legend, the reader is referred to the web version of this article.)

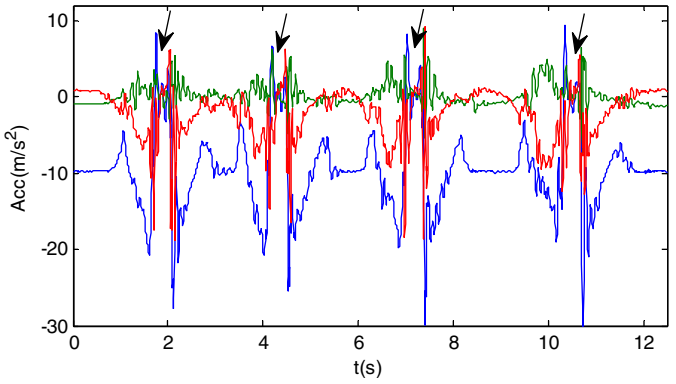

Fig. 17. Root accelerometer measurement while jumping.

Table 2
Accuracy in different motions.

Item		Walking (%)	Jumping & running (%)
Velocity	V-SLAC	<1	1–2
	A-SLAC	2	3
Position	V-SLAC	<1	1–2
	A-SLAC	1–2	2

From Figs. 15 and 16, the velocity and location data from the integration (dashed-line) drifts quickly only several seconds after the motion starts. Through eliminating the acceleration errors in A-SLAC, the drifting issue of the velocity and the position is eliminated. The tracked running distance matches nicely with the reference distance (7.5 m). The location error for each cycle is about 10 cm with the total distance of 15 m.

This jogging distance is still too short for evaluating the system in daily jogging exercise. Further study on longer distance outdoor jogging will be tested in the future.

4.4. Analysis

In dynamic motions like running and jumping with flying phases with no reference velocity, the velocity is also updated from the integration of the estimated root acceleration. It is discussed that the measurement during dynamic motions is not as accurate as during static motions [1,3]. However, it is noted that during the flight phases, the measured special force (f) by the accelerometer of the root IMU is near trivial (As shown in Fig. 17, during the flight phase, f is very small with RMS less than 2 m/s^2 while jumping and jogging). This is because of the fact that the root point is near to the average CG point of the person whose acceleration is exactly g during flight phase. Thus, from Eq. (3), we know that the acceleration bias (δa) error is also near trivial. Thus, the velocity can be update by integrating the root acceleration during the short flight duration. The slight errors can be corrected soon once the reference velocity shows up. Therefore, this method is useful for both slow and fast motion.

Based on the results of this paper and Ref. [3], the accuracies of V-SLAC and A-SLAC are listed in Table 2. A-SLAC uses only 3 IMUS as compared with eight IMUS in V-SLAC method. Although the accuracy is slightly lower, it is more convenient and costs less. The accuracy is acceptable for daily exercises.

5. Conclusion

This paper introduces a 3D velocity and position tracking method for human daily sports and practice applications using only 3 IMU sensors.

Based on an acceleration fine tuning method and human kinematics, the accurate and drift-free velocity result is achieved. The location of the human is also tracked based on this velocity and the human kinematics.

The system is able to track the velocity and the location of the person in both slow motions and dynamic motions with flight phases. Sports like: walking, jumping, jogging etc. can be accurately tracked based on this method.

The velocity and localization accuracy is evaluated using the commercial optical capture system. Velocity RMS errors can be less than 0.1 m/s for normal walking and jumping. The localization accuracy is within 2% of the total travelled distance.

In this system, no external assistive absolute positioning device is required, and it is convenient to wear on the body. There are no volume limitation or occlusion problems. These characteristics makes this system superior in applications in our daily activities or sports which happens in large and open terrains.

The accuracy of the proposed method can be improved based on more robust new IMU tracking algorithm and better MEMS sensor components. Therefore, applications in more highly dynamic sports tracking can be expected in the future.

Acknowledgments

This work was supported in part by the Agency for Science, Technology and Research, Singapore, under SERC Grant 12251 00005 and the Singapore Millennium Foundation Research Grant. The authors would like to thank the technical supports received from Dr. Albert, Mr. WS Ang, Mr. S.L. Teguh, Ms. LL Liu, Mr. BB Li, Ng Charles etc.

References

[1] M.A.D. Brodie, Development of fusion motion capture for optimization of performance in alpine ski racing, in: Ph.D. Thesis, Massey University, Massey, 2009.
[2] D. Vlasic, R. Adelsberger, G. Vannucci, J. Barnwell, M. Gross, W. Matusik, et al., Practical motion capture in everyday surroundings, ACM Trans. Graphics (TOG) 26 (2007) 35–44.
[3] Q. Yuan, I.-M. Chen, Human Velocity and Dynamic Behavior Tracking Method for Inertial Capture System, Sensors and Actuators A: Physical, 183 (01) (2012) 123–131.
[4] Qilong Yuan, I.-M. Chen, Simultaneous localization and capture with velocity information, in: IEEE/RSJ International Conference on Intelligent Robots and Systems, San Francisco, CA, 2011.
[5] E. Foxlin, Pedestrian tracking with shoe-mounted inertial sensors, IEEE Comput. Graphics Appl. 25 (2005) 38–46.
[6] P. Esser, H. Dawes, J. Collett, K. Howells, IMU: inertial sensing of vertical CoM movement, J. Biomech. 42 (2009) 1578–1582.
[7] Q. Li, M. Young, V. Naing, J. Donelan, Walking speed estimation using a shank-mounted inertial measurement unit, J. Biomech. 43 (2010) 1640–1643.
[8] M. Kourogi, T. Kurata, Personal positioning based on walking locomotion analysis with self-contained sensors and a wearable camera, in: Proceedings of the Second IEEE/ACM International Symposium on Mixed and Augmented Reality, Washington, DC, USA, 2003, pp. 103–112.
[9] G. Lachapelle, S. Godha, M. Cannon, Performance of integrated HSGPS-IMU technology for pedestrian navigation under signal masking, in: Proceedings of European Navigation Conference, Manchester, UK, 2006, pp. 8–10.
[10] L. Ojeda, J. Borenstein, Non-GPS navigation with the personal dead-reckoning system *Proc. SPIE* 6561, Unmanned Systems Technology IX, 65610C (May 02, 2007).
[11] E. Foxlin, S. Wan, Improved pedestrian navigation based on drift-reduced MEMS IMU chip, in: Proceedings of the 2010 ION International Technical Meeting, 2010.
[12] Qilong Yuan, I.-M. Chen, S.P. Lee, SLAC: 3D localization of human based on kinetic human movement capture, in: 2011 IEEE International Conference on Robotics and Automation (ICRA), Shanghai, China, 2011.
[13] Qilong Yuan, I.-M. Chen, 3D localization of human based on inertial capture system, IEEE Trans. Rob. 29 (3) (2013) 806–812.
[14] Qilong Yuan, I.-M. Chen, A.W. Sin, Method to calibrate the skeleton model using orientation sensors, in: 2013 IEEE International Conference on Robotics and Automation (ICRA), Karlsruhe, Germany, 2013.
[15] S. Kajita, F. Kanehiro, K. Kaneko, K. Yokoi, H. Hirukawa, The 3D linear inverted pendulum mode: a simple modeling for a biped walking pattern generation, in: Proceedings of IEEE/RSJ International Conference on Intelligent Robots and Systems, Maui, HI, 2001, pp. 239–246.

[16] APDM. (2013) www.apdm.net
[17] InterSense. (2013). *www.intersense.com*.
[18] G. Welch, G. Bishop, An Introduction to the Kalman Filter, 1995, pp. 1–16.
[19] R. Kalman, A new approach to linear filtering and prediction problems, J. Basic Eng. 82 (1960) 35–45.
[20] E. Bachmann, Inertial and magnetic tracking of limb segment orientation for inserting humans into synthetic environments, in: Ph.D. Thesis, Naval Postgraduate School, Monterey, CA., 2000.
[21] D. Roetenberg, Inertial and magnetic sensing of human motion, in: Ph.D. Thesis, Universiteit Twente, Enschede, 2006.

Biographies

Qilong Yuan received the bachelor degree in mechanical engineering and automation from Shanghai Jiao Tong University, Shanghai, China, in 2009. He did his Ph.D. degree at Nanyang Technological University (NTU), Singapore from 2009 to 2013. Mr. Yuan is currently a research engineer in Robotics Research Center, School of Mechanical and Aerospace, NTU. His research interest is in human motion tracking, inertial sensors, industrial robotics and humanoid robotics.

Prof. I-Ming Chen, Fellow of IEEE and Fellow of ASME, received the B. S. degree from National Taiwan University in 1986, and M. S. and Ph. D. degrees from California Institute of Technology, Pasadena, CA in 1989 and 1994 respectively. He has been with the School of Mechanical and Aerospace Engineering of Nanyang Technological University (NTU) in Singapore since 1995. He is currently Director of Robotics Research Center in NTU, and also Director of Intelligent Systems Center in NTU, a partnership between Singapore Technology Engineering Ltd. and NTU. His research interests are in wearable sensors, human-robot interaction, reconfigurable automation, and parallel kinematics machines (PKM). Prof. Chen has published more than 260 papers in refereed international journals and conferences as well as book chapters. He had been the technical editor of IEEE/ASME Transactions on Mechatronics (2003-2009) and IEEE Transactions on Robotics (2006-2011). Currently he is Associate Editor of Mechanism and Machine Theory and Editorial Board Member of Robotica, He was General Chairman of 2009 IEEE/ASME International Conference on Advanced Intelligent Mechatronics (AIM2009) in Singapore and 2013 IFToMM International Symposium on Robotics and Mechatronics (ISRM 2013) in Singapore. He will be General Chairman of 2017 IEEE International Conference on Robotics and Automation (ICRA 2017) in Singapore.